Materials Physics and Mechanics 37 (2018) 140-145 Received: December 22, 2017

ELECTRICAL CONDUCTIVITY OF THE NANOCOMPOSITE LAYERS FOR USE IN BIOMEDICAL SYSTEMS

L.P. Ichkitidze[1,2]*, A.Yu. Gerasimenko[1,2], V.M. Podgaetsky[1], S.V. Selishchev[1], A.A. Dudin[3], A.A. Pavlov[3]

[1]National Research University of Electronic Technology, bld. 1, Shokin Square, Zelenograd, Moscow, 124498, Russia

[2]I.M. Sechenov First Moscow State Medical University, bld. 4, Bolshaya Pirogovskaya Str., 2, Moscow, 119991, Russia

[3]Institute of Nanotechnology and Microelectronics of the Russian Academy of Sciences bld. 11, Nagatinckaia Str., 16a, Moscow, 115487, Russia

*e-mail: ichkitidze@bms.zone

Abstract. Nanocomposite layers consisting of an acrylic paint and single-walled carbon nanotubes (~1.5 wt.%) have been investigated. The investigated samples had a disk shape with a diameter of 20 – 30 mm and a thickness of 2 – 50 μm. After exposure in water for 350 h, the layer mass remained almost invariable (a mass loss of $\leq$ 1.5%) and the layer samples exhibited high adhesion to glass substrates and a conductivity of ~ 40 S/m. The layers consisting of the nanotubes and acrylic paint exfoliated from the substrates for ~1 h. After heat treatment at a temperature of 140 °C, all the layers exhibited a semiconductor-type temperature dependence of the resistance. The prospects of using these layers in various medical products, e.g. implants for wireless energy transmission, have been discussed.
Keywords: acrylic paint; carbon nanotubes; nanocomposite layers; electrical conductivity.

1. Introduction

Carbon nanotubes (CNTs) have the unique properties, including the high strength, electrical and thermal conductivities. The nanocomposites, containing CNTs, have the high potential of application in biomedical systems, since even a minor CNT content ($C \leq 2$ wt.%) leads to the unique properties of these materials.

Of particular interest are biomaterials and biocompatible materials with the low C values [1]. In a nanomaterial made of plasticized starch and multi-walled CNTs (MWCNTs), the double tensile strength and Young's modulus values were found [2]. The similar variation was observed in chitosan [3] and albumin [4 – 6]. Meanwhile, the nanomaterials were characterized by the minor C values: 2 wt.% in [3], 3 wt.% in [4], and $\leq$ 0.1 wt. % in [4 – 6]. A polymer (polyurethane) matrix, filled with MWCNTs, exhibited the percolation threshold at C = 0.13 wt.% [7, 8] and a carboxymethylcellulose (CMC) matrix, the percolation threshold at a level of C = (0.1 – 0.25) wt.% of MWCNTs [8].

In type-I collagen, a 2-wt.% single-walled CNT (SWCNT) addition increases the conductivity of the material by several orders of magnitude (to $\sigma \sim$ (1.2 – 1.6) S/m [9]); in carrageenan and chitosan with 0.6 wt.% of SWCNTs, the σ value increases by six orders of magnitude and attains 3200 S/m [10].

http://dx.doi.org/10.18720/MPM.3722018_5

In the combinations of various biological materials (hyaluronic acid, chitosan, heparin, gelatin, spermidine, albumin, carrageenan, CMC, etc.) and CNTs in a concentration of higher than 20 wt.%, the conductivities $\sigma \geq 1$ kS/m can be obtained at the preferred unidirectional CNT orientation. The high conductivities (σ ~ 50 kS/m) were implemented in the nanocomposite layers, consisting of a CMC matrix from a biocompatible material and MWCNT or SWCNT fillers (1 – 5 wt.%) exposed to laser radiation and treated at temperatures of ≥ 300 °C [8, 11]. The nanocomposites, based on biomaterials and biocompatible materials, most frequently demonstrated the conductivity values acceptable for the development of different medical devices (electrodes for electrocardiographs and electroencephalographs, implants, etc.). However, they are often unstable in water and moist environment [9 – 11], which strongly limits their application in medicine.

In this work, we investigate the electrical conductivity of nanocomposite layers consisting of an acrylic paint matrix, filled with SWCNTs.

In the present work, the electrical conductivity of layers of composite nanomaterials is investigated in the matrix – acrylic paint and filler – single-walled nanotubes.

2. Samples and experimental methods

Single-walled carbon nanotubes were formed by arc-driven synthesis and had a diameter of ~1.5 nm and a length of ≥ 1 μm [13]. The carboxylated (functionalized) SWCNTs in the form of a thick aqueous dispersion (paste) are offered for sale. Some of their parameters are given in Table 1.

Table 1. Some parameters of SWCNT.

Manufactures	NPF OOO "Uglerod ChG" [13]
View	Powder (purity ≥ 95 %)
Concentration of SWCNT	2.5 %
Density, g/cm^3	1.7 – 1.9
Bulk density, kg/m^3	0.1
Specific surface, m^2/g	~ 200 – 400

It can be seen that the SWCNT volume content is high (≥ 95%). It should be emphasized that the specific surface of individual SWCNTs is ~1300 m^2/g; however, since they are highly aggregated, their specific surface amounts to (200 – 400) m^2/g. Then, the average nanotube strands can attain 5 – 15 nm in diameter and 1 – 10 μm in length.

Figure 1 shows electron microscopy images of the layer consisting of only nanotubes. One can see different SWCNT strands with a maximum thickness of several tens of nm.

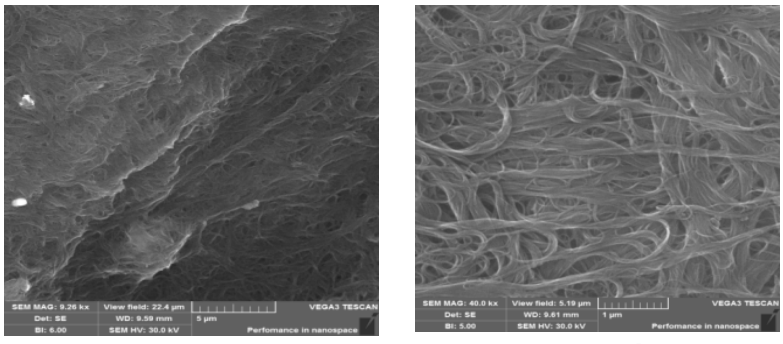

a *b*

Fig. 1. Electron-microscope images of films from SWCNT, scales: *a* – 5 μm; *b* – 1 μm.

The nanomaterial matrix was an acrylic paint (AP) (TU2331-034-05751640-2006) added with SWCNTs. The AP/SWCNT suspension was thoroughly mixed in a magnetic stirrer for 24 h and dispersed in a Qsonica Q700 ultrasonic disperser for 30 min. Before deposition onto substrates, the suspension was processed in an ultrasonic bath for 60 min.

The suspension contained 50 wt.% of the AP and 50 wt.% of the SWCNT paste and was characterized by the high viscosity (up to the glycerine level). The suspension was deposited by silk screening onto the substrates made of polyethylene terephthalan (PET, Petri dishes, or plates with thicknesses from 0.1 to 0.3 mm), and glass. The samples were disks with a diameter of 20 – 30 mm and a thickness of 2 – 50 μm. The typical samples, formed in a Petri dish, are shown in Fig. 2. The AP used had blue colour, so the layers prepared from the AP/SWCNT suspension acquired a black colour with a slight shade of blue.

The three sample groups were prepared: AP layers (group I), SWCNT layers (group II), and AP/SWCNT layers (group III). Three layers were deposited on the substrates of each type; each sample group included six sample layers.

It is important to estimate the composition of dried AP/SWCNT nanocomposite layers. For this purpose, we measured a solvent mass loss in the prepared layers, i.e., masses m_l and m_d of the indicated layers on glass and PET substrates in the liquid and dried states, respectively. The mass loss with respect to the mass in the liquid state (m_l) was determined as $m_w = (m_l - m_d)/m_l$. The obtained average values are m_w = 52% for group-I samples, 97.1% for group-II samples, and 51% for group-III samples. The SWCNT masses in the dried layers (100 – 97.1)% = 2.9% (group II), obtained by us, are similar to a nanotube relative mass of 2.5% in the paste, presented by the manufacturer (Table 1). Using the obtained m_w data, we found the dried nanocomposite layer composition to be 95 wt.% AP/5 wt.% SWCNTs.

Fig. 2. Appearance of AP/SWCNT layers in Petri dishes.

The dependence of resistance R on temperature t was measured in a thermostat in the temperature range of t ~ 20 – 200 °C. The temperature growth (drop) rate was controlled in the range of (0.5 – 1.0)°C/min. The specified temperature was held with an accuracy of ±1°C.

The sample resistance was measured by a two- or four-probe method. All the electrical measurements were performed in the current source mode. To do this, strip and square samples were prepared. The resistivity and conductivity of the samples were determined from their geometrical sizes and resistance.

3. Results and discussion

For all the sample groups, the layer mass loss was controlled after multiple immersions of the samples in water with the subsequent drying. The samples were immersed in water and kept there for 1, 12, 48, 96, and 192 h. Each time, the samples were taken from water, dried, and weighed. The total time of exposure in water was ~350 h. This experiment was carried out for

the layers deposited onto glass substrates. After ~1 h of exposure in water, the AP and SWCNT layers (group-I and II samples) exfoliated from the substrates, but the mass loss experiments were continued. The AP/SWCNT nanocomposite layers remained on the substrates throughout the experiment without changing the appearance and reducing the degree of adhesion to the glass substrates. The analogous behavior of mass loss in water was observed for the layers deposited on PET substrates.

The total layer mass loss relative to the initial mass after the last immersion and drying was 3% for group-I samples and 1.63% for group-III samples, while the layers of the group-II samples were completely destructed. Thus, the AP layers are easily destructed and lose their mass in water faster than the AP layers with small SWCNT additions (the nanocomposite 95 wt.% of AP/5 wt.% of SWCNTs). Meanwhile, the adhesion of the AP/SWCNT layers is higher than that of the AP layers.

Figure 3 shows breakage patterns of the AP/SWCNT nanocomposite layer. One can clearly see carbon nanotubes uniformly distributed in the bulk of the sample (Fig. 3a) and nanotube strands (Fig. 3b). Nanotubes are connected with each other, which can be important for the electric current flow in the investigated material.

The resistance variation with temperature for the group-I samples was not recorded, since their resistances were beyond the capability of a measuring device (200 MΩ). This value, recalculated to the conductivity with regard to geometrical sizes, was found to be ~10^{-4} S/m.

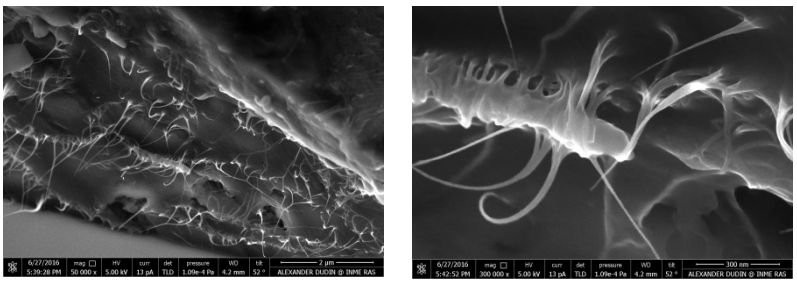

a *b*

Fig.3. Electron-microscopic images of the AP/SWCNT layer, scales: *a* – 1 μm; *b* – 300 nm.

Figure 4 shows typical temperature dependences of $R(t)/R_0$ for the group-II and III samples; $R(t)$ is the resistance variation with temperature and R_0 is the sample resistance at the beginning of heating. The values and qualitative behaviour of the curves depended on the measurement mode (heating or cooling). In particular, for group-II and III samples No. 1 on glass substrates, we obtained R_0 = 0.81 Ω and R_0 = 1016 Ω, respectively, at t = 22 °C (Fig. 4a). During heating, different behaviours of the curves are observed: metallic for the nanotube layers (group II) and semiconductor for the nanocomposite layers (group III). During cooling, the layers of both groups exhibit the semiconductor behaviour. In addition, the conductivities σ_0 of the samples, calculated from the R_0 data and geometrical sizes, were found to be strongly different: σ_0 ~ 20 kS/m for group-II samples and σ_0 ~ 15 S/m for group-III samples.

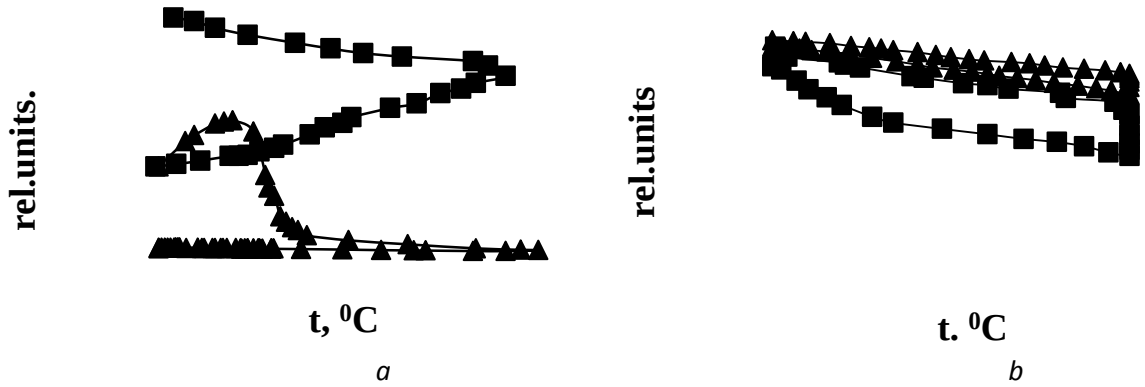

Fig. 4. Temperature dependences of the resistance of the layers: (a) sample No.1, the first heating, ▲ – AP/SWCNT layers, ■ – SWCNT; (b) sample 2, the third heating, annealing, cooling, ▲ – AP/SWCNT layers, ■ – SWCNT.

The $R(t)/R_0$ curves of the AP/SWCNT layers contain the maximum at a temperature of $t \approx 45$°C, which disappears during sample reheating or annealing. The similar maximum for the nanocomposite layers, containing MWCNTs, was attributed to structural defects, contained in nanotubes [14].

Figure 4b shows the $R(t)/R_0$ curves for group-II and III samples No. 2 on glass substrates at t = 23 °C and R_0 = 0.68 Ω (σ_0 ~ 25 kS/m, group II) and R_0 = 495 Ω (σ_0 ~ 40 S/m, group III). The layers were subjected to the second heating/cooling cycle. The samples of both these groups were held at t = 140 °C for 6 h, which is shown in the $R(t)/R_0$ curves by vertical lines. It can be seen that the resistance of the group-II layers increases by a factor of more than 3 and the resistance of the group-III layers decreases by ~20% relative to the initial R_0 values.

It should be noted that the value of σ_0 ~ 40 S/m for the AP/SWCNT nanocomposite layers (group III) differs from the value of $\sigma_0 \leq 10^{-4}$ S/m of the initial AP material (group I) by more than five orders of magnitude. The $R(t)/R_0$ hysteresis upon numerous heating/cooling cycles of the samples from this group is insignificant (Fig. 3b). In particular, the maximum hysteresis $2[R(\uparrow) - R(\downarrow)]/[R(\uparrow) + R(\downarrow)]$ is no higher than 8%. Here, $R(\uparrow)$ and $R(\downarrow)$ are the sample resistances with increasing and decreasing temperature, respectively. For both group-II and III layers, the $R(t)/R_0$ curves after the second and next heating/cooling cycles exhibited only the semiconductor-type behaviour similar to that shown in Fig. 4b for the AP/SWCNT layer. In this case, the $R(t)/R_0$ hysteresis of the SWCNT layers was significant (≥ 30%).

The $R(t)$ behaviour of σ_0 value (in the order of magnitude) for the group-II and III samples can be related to the following circumstance. The effect of temperature and heat treatment in air leads to the formation of defects and the contact resistance growth at the contact points between CNTs. This stimulates the resistance growth and changes the metal-type conductivity for the semiconductor-type one in the group-II layers (SWCNTs). The heat treatment of group-III (AP/SWCNT) layers apparently reduces the average thickness of tunnel contacts between nanotubes. In this case, the nanotubes are located inside the composite and not exposed to air. Consequently, the contact resistance between them and the resistance of the layer decreases. Indeed, the conductivity model of a matrix with randomly distributed CNTs explains qualitatively an increase in the matrix conductivity with a decrease in the contact resistance between nanotubes.

4. Conclusion

Thus, we experimentally investigated the electrical conductivity of nanocomposite layers with a thickness of 2 – 50 μm. The nanocomposite consisted of an acrylic paint matrix, filled with single-walled carbon nanotubes. The main results of this study are:

- the high degree of adhesion of the layers to the glass substrates and low mass loss after exposure in water for 350 h;
- the high conductivity limit (~ 40 S/m) at the low nanotube content (95 wt.% AP/5 wt.% SWCNT) in the layers, which is higher than the conductivity of the initial acrylic paint material by more than 5 orders of magnitude;
- a decrease in the layer resistance and change of the temperature dependence of the resistance for the semiconductor type upon multiple heating/cooling cycles and heat treatment at a temperature of 140 °C;
- insignificant (≤ 8%) hysteresis of the temperature dependence of the resistance upon multiple heating/cooling cycles.

The electrical conductivity of the material is a decisive parameter in operation of most modern systems and sensors. In view of this, the investigated conducting nanocomposite layers are promising for applications as functional nanomaterials. They can be used, for example, as biomedical electrodes for body electronics and electrocardiography, elastomers for general and biomedical purposes (strain gauges, artificial muscle, etc.), and electroconductive systems for wireless energy transmission in body implants.

Acknowledgement. *This work was provided by the Ministry of Education and Science of the Russian Federation (Grant 20.9216.2017/6.7).*

References

[1] J.M. Tan, P. Aruselvan, S. Fakurazi et al. // *Jour. of Nanomaterials* **20** (2014) 917024.
[2] X. Cao, Y. Chen, P.R. Chang, M.A. Huneault // *Journal of Applied Polymer Science* **106** (2007) 1431.
[3] S.F. Wang, W.D. Zhang , Y.J. Tong // *Biomacromolecules* **6(6)** (2005) 3067.
[4] L.P. Ichkitidze, S.V. Selishchev, A.Yu. Gerasimenko, V.M. Podgaetsky // *Biomedical Engineering* **49(5)** (2016) 308.
[5] S.A. Ageeva, V.I. Eliseenko, A.Yu. Gerasimenko, L.P. Ichkitidze et al. // *Biomedical Engineering* **44(6)** (2011) 233.
[6] L.P. Ichkitidze, V.M. Podgaetsky, O.V. Ponomareva, S.V. Selishchev // *Izvestia VUZov Fizika* **3/2** (2010) 125 (In Russian).
[7] R. Zhang, A. Dowden, M. Baxendale, T. Peijs // *Composite Science and Technology* **69(10)** (2009) 1499.
[8] L.P. Ichkitidze, V.M. Podgaetsky, A.S. Prihodko et al. // *Biomedical Engineering* **47(2)** (2013) 68.
[9] C.M. Voge, M. Kfriolis, R.A. MacDonald, J.P. Stegemann // *Journal of Biomedical Materials Research* **86A(1)** (2008) 278.
[10] A.J. Granero, J.M. Razal, G.G. Wallace, M. Panhuis // *Journal of Materials Chemistry* **20(37)** (2010) 7953.
[11] L.P. Ichkitidze, S.V. Selishchev, A.Yu. Gerasimenko et al., *Patent RU* 2473368, 27.01.2013 (In Russian).
[12] J.Xu, W. Florkowski, R. Gerhardt et al. // *J. Phys. Chem. B* **110** (2006) 12289.
[13] A.V. Krestinin, A.P. Kharitonov, Yu.M. Shul'ga et al. // *Nanotechnologies in Russia* **4(1-2)** (2009) 60.
[14] A.A. Babaev, A.M. Aliev, E.I. Terukov, A.K. Fillipov // *High Temperature* **55(4)** (2017) 502.